



## Accurate computation of wave loads on a bottom fixed circular cylinder

**Paulsen, Bo Terp; Bredmose, Henrik; Bingham, Harry B.**

*Published in:*  
International Workshop on Water Waves and Floating Bodies

*Publication date:*  
2012

*Document Version*  
Publisher's PDF, also known as Version of record

[Link back to DTU Orbit](#)

*Citation (APA):*  
Paulsen, B. T., Bredmose, H., & Bingham, H. B. (2012). Accurate computation of wave loads on a bottom fixed circular cylinder. In *International Workshop on Water Waves and Floating Bodies*

---

### General rights

Copyright and moral rights for the publications made accessible in the public portal are retained by the authors and/or other copyright owners and it is a condition of accessing publications that users recognise and abide by the legal requirements associated with these rights.

- Users may download and print one copy of any publication from the public portal for the purpose of private study or research.
- You may not further distribute the material or use it for any profit-making activity or commercial gain
- You may freely distribute the URL identifying the publication in the public portal

If you believe that this document breaches copyright please contact us providing details, and we will remove access to the work immediately and investigate your claim.

# Accurate computation of wave loads on a bottom fixed circular cylinder

B. T. Paulsen<sup>\*,1</sup>, H. Bredmose<sup>†</sup>, H. B. Bingham<sup>\*</sup>

<sup>\*</sup>Technical University of Denmark, Department of Mechanical Engineering,  
Lyngby, Denmark

<sup>†</sup> Technical University of Denmark, Department of Wind Energy, Lyngby, Denmark  
E-mail: botp@mek.dtu.dk, hbr@mek.dtu.dk, hbb@mek.dtu.dk

## Background

This abstract describes recent progress in the development of a fast and accurate tool for computations of wave-structure interactions of realistic sea states that include breaking waves. The practical motivation is extreme wave loads on offshore wind turbine foundations, but the tool is applicable to a range of other problems.

The central idea is to drive an inner CFD model that resolves the flow around the structure with an outer wave model that is based on potential flow theory. By letting the potential flow solver describe the waves in the outer flow domain and the Navier-Stokes solver describe the flow in the inner domain a fast and accurate description of wave loads on offshore structures is obtained, even for breaking waves.

Engsig-Karup et. al [1] have recently developed a fully nonlinear potential flow solver (OceanWave3D) to represent propagation and development of fully nonlinear three-dimensional water waves up to the point of breaking.

The CFD solver is the open source CFD toolbox OpenFOAM® in combination with the newly developed waves2Foam utility, which in [5] has been successfully applied to calculations of free surface flows. The numerical solution is obtained by solving the incompressible Navier-Stokes equations in combination with a surface tracking scheme. The CFD solver has been thoroughly tested for stability and first order grid convergence has been shown for the propagation of stream function waves.

Here we present results for the magnitudes, of the third-harmonic forces on a vertical circular cylinder from steep waves. This partly serves as a validation and further brings insight into third-harmonic wave loads on cylinders which are relevant for ringing. Next, preliminary results for the coupled model are presented in terms of irregular waves propagation and the associated forces on a cylinder.

## Higher-harmonic wave loads on a circular cylinder at finite water depth

With the use of the CFD model wave loads on a circular cylinder with radius,  $R = 3\text{m}$ , at a finite water depth of  $h = 30\text{m}$  are investigated. The incompressible Navier-Stokes equations are solved by a finite-volume method for the two-phase flow of water and air. A Volume of Fluid (VOF) scheme is applied for the representation of the free surface. For all computations, regular two-dimensional stream function waves [3] with wave number  $k$ , radian frequency  $\omega$  and amplitude  $A$  are applied as incident waves.

---

<sup>1</sup>Presenting author

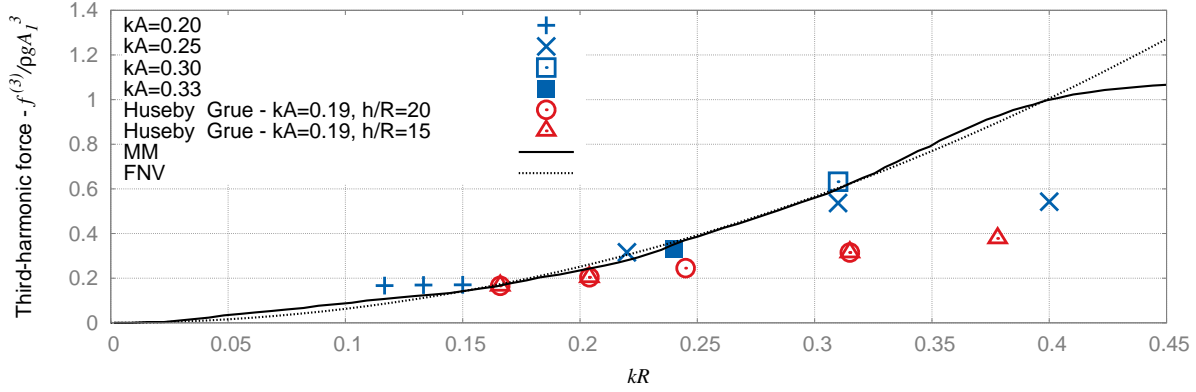


Figure 1: The magnitude of the third-harmonic wave force on circular cylinder. Blue symbols indicate third-harmonic forces from the numerical calculations. Red symbols indicate experimental results by Huseby & Grue [4]. For all calculations  $h/R = 10$

When the bottom mounted cylinder is exposed to a field of incident waves, it is subjected to a depth-integrated force,  $F(t)$ , which can be written as,

$$F(t) = \Re \left\{ f^{(1)} e^{i\omega t} + f^{(2)} e^{i2\omega t} + f^{(3)} e^{i3\omega t} + \dots \right\} \quad (1)$$

where  $i = \sqrt{-1}$  is the complex unit and  $f^{(j)} = f^{(j)}(kh, kR, kA)$  is the magnitude of the  $j$ th force component. The magnitude of the  $j$ th force component is made dimensionless by  $\rho g A_1^3$  where  $\rho$  is the density of water,  $g$  is the acceleration of gravity and  $A_1$  is the first component of the Fourier series representing the incident free surface elevation, given by the stream function solution.

The numerically calculated third-harmonic force,  $f^{(3)}$ , is presented in figure 1 as a function of the relative cylinder diameter,  $kR$ . The theoretical results of Faltinsen, Newman and Vinje (FNV) [2] and Malenica and Molin (MM) [7] are shown as a dashed and a solid line respectively. Finally, in the figure, experimental results by Huseby & Grue [4] are shown for comparison. The comparison with the experimental results is not complete since the relationship between the water depth and the cylinder radius applied in the experiments was either  $h/R = 20$  or  $h/R = 15$ , while  $h/R = 10$  was used in the numerical calculations and the results by MM. Notice that the only results presented by MM are for  $h/R = 10$ . Therefore this ratio was adopted in the numerical calculations to make a comparison possible. The analytic solution by FNV is formulated at infinite water depth and is therefore independent of the  $h/R$ -ratio.

In figure 1 a good agreement between the numerically predicted values of  $f^{(3)}$  and the theories by FNV and MM is seen for  $kR < 0.35$ . For values of  $kR > 0.35$  the numerically computed third-harmonic forces are smaller than predicted by the theories. However, this discrepancy is in agreement with experiments of Huseby & Grue [4] and Krokstad et. al. [6], who, likewise, observed discrepancies between experimental results and the theories for larger values of  $kR$ .

## Irregular wave loads on a bottom fixed circular cylinder at finite water depth

The combined potential flow- and Navier-Stokes solver is used to analyse hydrodynamic forces from irregular waves on a circular cylinder. Forces calculated with the Morison equation, given kinematics from the potential flow model, are compared with forces calculated by the potential-flow-driven Navier-Stokes solver.

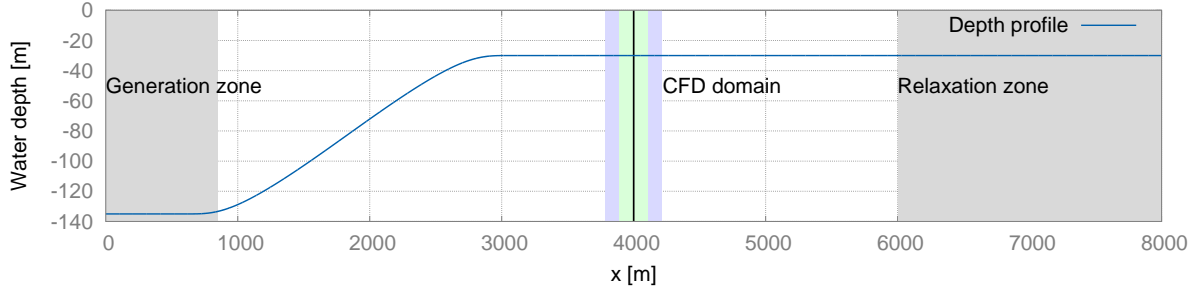


Figure 2: Physical and computational domain for irregular wave computations. Generation and relaxation zones are indicated by shaded grey. The computational domain of the Navier-Stokes solver is indicated with shaded green and the generation relaxation zones are indicated with blue.

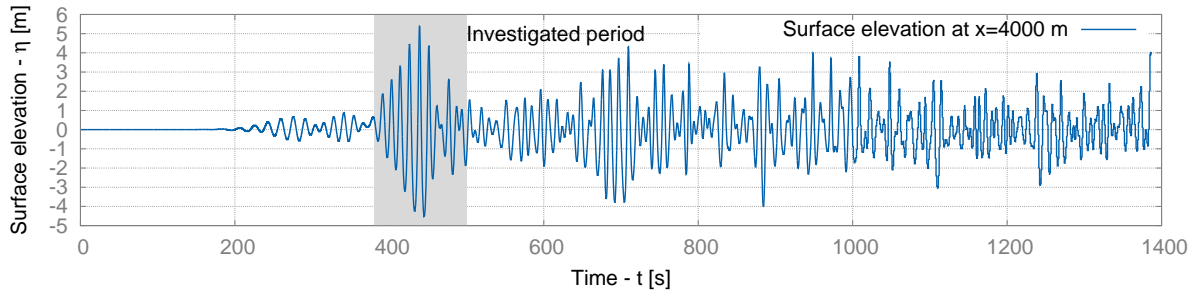


Figure 3: The surface elevation calculated by the potential flow model at the position of the cylinder,  $x = 4000\text{m}$ .

In order to drive the Navier-Stokes solver, a one-way coupling between the potential flow model and the Navier-Stokes solver has been developed and incorporated into the interface of the waves2Foam utility [5]. At the start of the CFD computations, information from the potential flow model is interpolated into the computational domain of the Navier-Stokes solver. Hereafter the two models are time stepped concurrently and the generation and absorption zones of the CFD model are, at every time step, fed with data from the potential flow model. This is efficient because the potential flow model is faster than the CFD solver and does therefore not add substantial computational overhead.

The combined model is applied to a case of unidirectional irregular JONSWAP waves of  $T_p = 12\text{s}$  and  $H_s = 8\text{m}$ . A sketch of the domain for the potential flow model is shown in figure 2. The waves are generated at  $h_0 = 135\text{m}$  and propagated by the potential flow model to a finite water depth of  $h_1 = 30\text{m}$ . The resulting free surface elevation at  $x = 4000\text{m}$  is shown in figure 3. The time series was visually inspected and the shaded period recalculated with the combined model. The computational domain of the Navier-Stokes solver had a size of  $\{L_x, L_y, L_z\} = \{650; 30, 40\}\text{m}$  and was resolved with  $\sim 300.000$  cells.

A simple estimate of the forces on the cylinder is provided by application of the Morison equation with kinematics from the potential flow model. While this approach allows a practical prediction of the forces from fully nonlinear waves, even for long time series (see e.g. [8]), the Morison approximation is limited to non-breaking waves with no severe run-up and slender cylinders. A more accurate calculation of the forces on the cylinder can be made by integrating the pressure on the cylinder, calculated by the Navier-Stokes solver. With this method the hydrodynamic forces can be calculated with the accuracy of the numerical approximation, even for violently breaking waves.

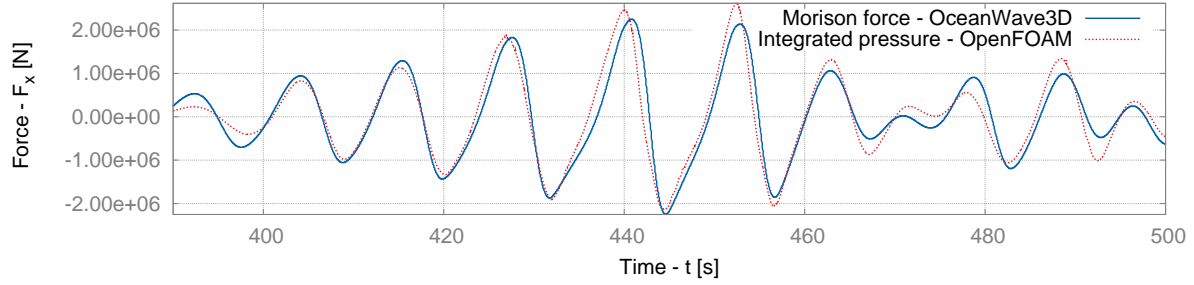


Figure 4: Depth integrated hydrodynamic force from irregular waves on a circular cylinder. Blue line represents forces based on the Morison equation and kinematics from the potential flow solver. Red line represents forces from the solution of the incompressible Navier-Stokes equations.

For the event indicated in figure 3, forces on the cylinder are calculated and presented in figure 4. Especially for the smaller waves in the beginning of the simulation an excellent agreement is seen. The discrepancy observed for the largest wave and hereafter is attributed to the effect of runup and the diffracted field.

Further application of the model will include breaking waves and multidirectional sea states. Comparison with experiments carried out at DHI, Denmark, will also be made.

## Acknowledgment

I would like to thank Signe Schløer and associate professor Allan Engsig-Karup for providing invaluable help with the running and analysing output from the potential flow solver, OceanWave3D. The research was supported by Energinet.dk as a part of the 'Wave Loads' project (ForskEL grant 10495).

## References

- [1] A.P. Engsig-Karup, H.B. Bingham, and O. Lindberg. An efficient flexible-order model for 3D nonlinear water waves. *Journal of Computational Physics*, 228(6):2100–2118, April 2009.
- [2] O.M. Faltinsen, J.N. Newman, and T. Vinje. Nonlinear Wave Loads On a Slender Vertical Cylinder. *Journal of Fluid Mechanics*, 289:179–198, April 1995.
- [3] J. Fenton. The numerical solution of steady water wave problems. *Computers & Geosciences*, 14(3):357–368, 1988.
- [4] M. Huseby and J. Grue. An Experimental Investigation Of Higher-Harmonic Wave Forces On a Vertical Cylinder. *Journal of Fluid Mechanics*, 414:75–103, July 2000.
- [5] N.G. Jacobsen, D.R. Fuhrman, and J. Fredsøe. A Wave Generation Toolbox For The Open-Source CFD Library: OpenFOAM. *International Journal for Numerical Methods in Fluids*, 2012. DOI: 10.1002/flid.2726.
- [6] J. R. Krokstad and C. T. Stansberg. Ringing Load Models Verified Against Experiments. In *OMAE*, pages 223–233, Copenhagen, 1995. ASME.
- [7] Š. Malenica and B. Molin. Third-Harmonic Wave Diffraction By a Vertical Cylinder. *Journal of Fluid Mechanics*, 302:203–229, April 1995.
- [8] S. Schløer, H. Bredmose, and H. B. Bingham. Irregular Wave Forces on Monopile Foundations: Effect of Full Nonlinearity and Bed Slope. In *International Conference on Ocean, Offshore and Arctic Engineering*. ASME, 2011.